NATIONAL ADVISORY COMMITTEE FOR AERONAUTICS

REPORT 1060

DETAILED COMPUTATIONAL PROCEDURE FOR DESIGN OF CASCADE BLADES WITH PRESCRIBED VELOCITY DISTRIBUTIONS IN COMPRESSIBLE POTENTIAL FLOWS

By GEORGE R. COSTELLO, ROBERT L. CUMMINGS, and
JOHN T. SINNETTE, Jr.

1952

REPORT 1060

DETAILED COMPUTATIONAL PROCEDURE FOR DESIGN OF CASCADE BLADES WITH PRESCRIBED VELOCITY DISTRIBUTIONS IN COMPRESSIBLE POTENTIAL FLOWS

By GEORGE R. COSTELLO, ROBERT L. CUMMINGS, and
JOHN T. SINNETTE, Jr.

Lewis Flight Propulsion Laboratory
Cleveland, Ohio

National Advisory Committee for Aeronautics

Headquarters, 1724 F Street NW., Washington 25, D. C.

Created by act of Congress approved March 3, 1915, for the supervision and direction of the scientific study of the problems of flight (U. S. Code, title 50, sec. 151). Its membership was increased from 12 to 15 by act approved March 2, 1929, and to 17 by act approved May 25, 1948. The members are appointed by the President, and serve as such without compensation.

JEROME C. HUNSAKER, Sc. D., Massachusetts Institute of Technology, *Chairman*

ALEXANDER WETMORE, Sc. D., Secretary, Smithsonian Institution, *Vice Chairman*

DETLEV W. BRONK, PH. D., President, Johns Hopkins University.

JOHN H. CASSADY, Vice Admiral, United States Navy, Deputy Chief of Naval Operations.

EDWARD U. CONDON, PH. D., Director, National Bureau of Standards.

HON. THOMAS W. S. DAVIS, Assistant Secretary of Commerce.

JAMES H. DOOLITTLE, Sc. D., Vice President, Shell Oil Co.

R. M. HAZEN, B. S., Director of Engineering, Allison Division, General Motors Corp.

WILLIAM LITTLEWOOD, M. E., Vice President, Engineering, American Airlines, Inc.

THEODORE C. LONNQUEST, Rear Admiral, United States Navy, Deputy and Assistant Chief of the Bureau of Aeronautics.

HON. DONALD W. NYROP, Chairman, Civil Aeronautics Board.

DONALD L. PUTT, Major General, United States Air Force, Acting Deputy Chief of Staff (Development).

ARTHUR E. RAYMOND, Sc. D., Vice President, Engineering, Douglas Aircraft Co., Inc.

FRANCIS W. REICHELDERFER, Sc. D., Chief, United States Weather Bureau.

GORDON P. SAVILLE, Major General, United States Air Force, Deputy Chief of Staff—Development.

HON. WALTER G. WHITMAN, Chairman, Research and Development Board, Department of Defense.

THEODORE P. WRIGHT, Sc. D., Vice President for Research, Cornell University.

HUGH L. DRYDEN, PH. D., *Director*

JOHN W. CROWLEY, JR., B. S., *Associate Director for Research*

JOHN F. VICTORY, LL. D., *Executive Secretary*

E. H. CHAMBERLIN, *Executive Officer*

HENRY J. E. REID, D. Eng., Director, Langley Aeronautical Laboratory, Langley Field, Va.

SMITH J. DEFRANCE, B. S., Director, Ames Aeronautical Laboratory, Moffett Field, Calif.

EDWARD R. SHARP, Sc. D., Director, Lewis Flight Propulsion Laboratory, Cleveland Airport, Cleveland, Ohio

TECHNICAL COMMITTEES

AERODYNAMICS
POWER PLANTS FOR AIRCRAFT
AIRCRAFT CONSTRUCTION

OPERATING PROBLEMS
INDUSTRY CONSULTING

Coordination of Research Needs of Military and Civil Aviation
Preparation of Research Programs
Allocation of Problems
Prevention of Duplication
Consideration of Inventions

LANGLEY AERONAUTICAL LABORATORY,
Langley Field, Va.

AMES AERONAUTICAL LABORATORY,
Moffett Field, Calif.

LEWIS FLIGHT PROPULSION LABORATORY,
Cleveland Airport, Cleveland, Ohio

Conduct, under unified control, for all agencies, of scientific research on the fundamental problems of flight

OFFICE OF AERONAUTICAL INTELLIGENCE,
Washington, D. C.

Collection, classification, compilation, and dissemination of scientific and technical information on aeronautics

REPORT 1060

DETAILED COMPUTATIONAL PROCEDURE FOR DESIGN OF CASCADE BLADES WITH PRESCRIBED VELOCITY DISTRIBUTIONS IN COMPRESSIBLE POTENTIAL FLOWS [1]

By George R. Costello, Robert L. Cummings, and John T. Sinnette, Jr.

SUMMARY

A detailed step-by-step computational outline is presented for the design of two-dimensional cascade blades having a prescribed velocity distribution on the blade in a potential flow of the usual compressible fluid. This outline is based on the assumption that the magnitude of the velocity in the flow of the usual compressible nonviscous fluid is proportional to the magnitude of the velocity in the flow of a compressible nonviscous fluid with linear pressure-volume relation. The computational procedure includes several ways of adjusting the prescribed velocity to satisfy restrictions imposed by the method. Tables of coefficients are given for evaluating the necessary integrals, including the determination of the harmonic conjugate function. Numerical examples are included.

INTRODUCTION

A method for computing blade profiles with prescribed velocity distributions based on the assumption that the pressure-volume relation is linear is presented in reference 1. The method uses the prescribed velocity distribution and compatible free-stream conditions to determine a mapping function that transforms an incompressible flow about the unit circle into an exact compressible flow, with linear pressure-volume relation, about a cascade of blades having the desired velocity distribution.

In order to apply this method to the design of a cascade with a given velocity distribution and free-stream conditions in a flow of an "actual" fluid (the usual compressible nonviscous fluid), the relation between the actual fluid and the fluid with the linear pressure-volume relation must be approximated so that the required velocity distribution and free-stream conditions for the second fluid may be determined. In this investigation, which was made at the NACA Lewis laboratory, the magnitudes of the velocities in the two fluids are assumed to be proportional and the constant of proportionality is determined by the continuity equation using the same upstream and downstream flow angles for the two fluids.

By use of this relation, a computational procedure was developed to obtain the blade profile with a minimum of effort. The procedure, presented herein, includes the adjustment of the prescribed velocity distribution to satisfy the restrictions on the mapping function and the numerical computation of the harmonic conjugate function.

SYMBOLS

The following symbols are used in this report:

$A, B, C_3, \ldots$ C_6, D	constants
a, b, c	constants
$C(e^{i\theta})$	function of θ defined by equation (18)
d	spacing of cascade blades
$H(e^{i\theta})$	function of θ
$\tilde{H}(e^{i\theta})$	final values of $H(e^{i\theta})$
Im	imaginary part
$K(\theta)$	distorted velocity defined by equation (22)
$\tilde{K}(\theta)$	modified $K(\theta)$
k	constant determined by range of potential
M	Mach number
n	constant determined by trailing-edge angle of blade
$Q(s)$	dimensionless velocity on blade in direction of increasing s
q	magnitude of dimensionless velocity (ratio of velocity to stagnation velocity of sound) for flow with linear pressure-volume relation
$\tilde{q}$	final value of q after modification of $Re H(e^{i\theta})$
Re	real part
$\Delta(ReH)$	change in $ReH(e^{i\theta})$
r	ratio of velocities (determined by equation (4))
s	arc length along blade measured counterclockwise from tail (figs. 1 and 2)
$\tilde{s}$	arc length along final blade shape
u	magnitude of dimensionless velocity (ratio of velocity to stagnation velocity of sound) for actual fluid
$v(\theta)$	velocity on unit circle (incompressible flow)
$z = x + iy$	complex variable in cascade plane
α	angle of velocity in compressible flow (measured from positive x-axis)
Γ	circulation (positive counterclockwise)
γ	ratio of specific heats
δ	difference between $Re\ H(e^{i\theta})$ and parabola at half-interval point
ϵ	including trailing-edge angle of blade
θ	circle angle (incompressible flow plane) positive counterclockwise

λ auxiliary function defined by equation (15)
ρ density
τ variable of integration
φ velocity potential

Subscripts:
c compressible flow
i incompressible flow
n leading edge (nose)
t trailing edge (tail)
1 upstream
2 downstream

RELATION BETWEEN FLOWS

In the present problem of designing a cascade, the prescribed conditions are the upstream velocity $u_1 e^{i\alpha_1}$, the downstream velocity $u_2 e^{i\alpha_2}$, and the magnitude of the dimensionless velocity on the blade as a function of the arc length $u=u(s)$ (see figs. 1 and 2). The upstream and downstream velocities are related by the continuity equation

$$\left(1-\frac{\gamma-1}{2}u_1^2\right)^{\frac{1}{\gamma-1}} u_1 \cos \alpha_1 = \left(1-\frac{\gamma-1}{2}u_2^2\right)^{\frac{1}{\gamma-1}} u_2 \cos \alpha_2 \qquad (1)$$

Consequently, only three of the quantities u_1, u_2, α_1, and α_2 may be assigned, and the fourth is determined by equation (1).

In utilizing the method of reference 1 to design the cascade, the prescribed conditions are employed to determine the upstream and downstream velocities and the velocity distribution on the blade for the fluid with the linear pressure-volume relation by assuming that the magnitudes of the velocities for the two flows are proportional; that is,

$$q=ru \qquad (2)$$

The constant of proportionality is determined from the additional assumption that the flows have the same free-stream directions by substitution of equation (2) in the
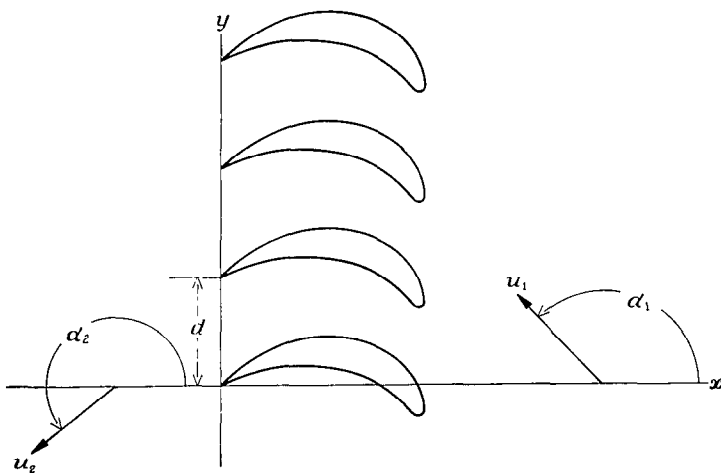
FIGURE 1.—Cascade in z-plane.
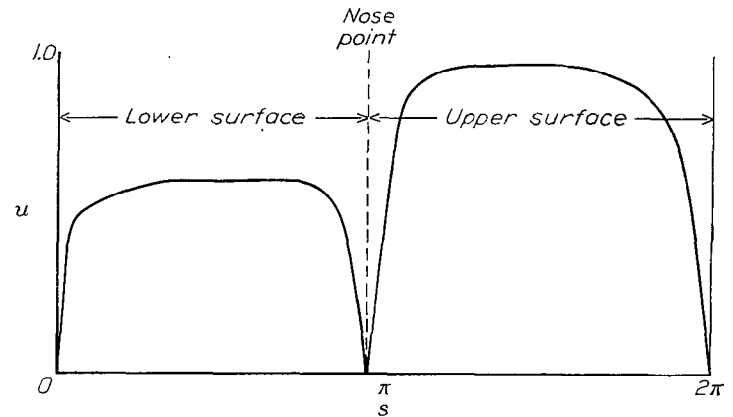
FIGURE 2.—Prescribed velocity distribution on cascade blade.

continuity relation for the flow with the linear pressure-volume relation:

$$\frac{1}{\sqrt{1+q_1^2}} q_1 \cos \alpha_1 = \frac{1}{\sqrt{1+q_1^2}} q_2 \cos \alpha_2 \qquad (3)$$

$$r^2 = \frac{u_2^2 \cos^2 \alpha_2 - u_1^2 \cos^2 \alpha_1}{u_1^2 u_2^2 (\cos^2 \alpha_1 - \cos^2 \alpha_2)} \qquad (4)$$

Hence, the upstream velocity $q_1 e^{i\alpha_1}$, the downstream velocity $q_2 e^{i\alpha_2}$, and the velocity distribution on the blade $q=q(s)$ are now determined for the flow with the linear pressure-volume relation.

Other approximations to the relation between the two flows could be used but, with the present cascade interpretation, the upstream and downstream flow angles and the spacing are the same for the two flows. The two density-velocity relations are also in good agreement, as shown in figure 3 where the density-velocity relations are plotted for $u_1=0.700$ and $u_2=0.500$. When the upstream and downstream velocities are equal, the density-velocity relation, as given by this interpretation, is the same as the density-velocity relation in the Kármán-Tsien approximation.
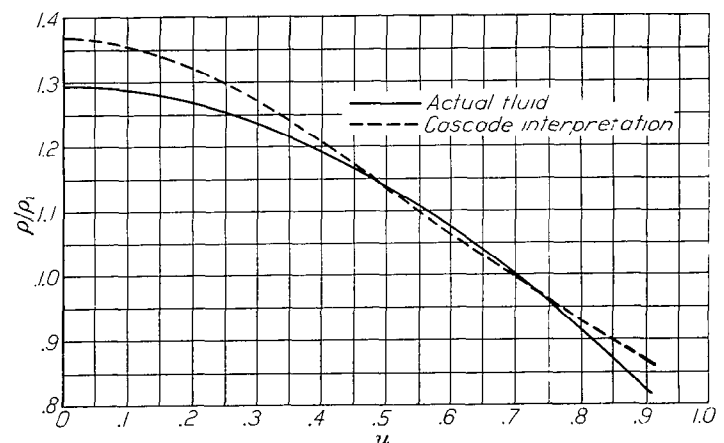
FIGURE 3.—Comparison of density-velocity relations for $u_1=0.700$ and $u_2=0.500$.

NUMERICAL PROCEDURE

After the free-stream conditions and velocity distribution on the blade are determined for the flow with the linear pressure-volume relation, the method of reference 1 is used to obtain the blade shape. In this method, the given conditions are used to select an incompressible flow about the unit circle and to determine the mapping function that transforms this flow into a compressible flow with the circle transforming into the desired blade. A detailed procedure for determining the circle flow and the mapping are given in the following paragraphs.

FLOW IN CIRCLE PLANE

The velocity potential $\varphi_c(s)$ and the circulation Γ_c on the blade are obtained by integrating the prescribed velocity distribution $q(s)$. For this purpose, it is convenient to define $Q(s)$ by

$$Q(s) = -q(s) \qquad 0 \leq s \leq s_n$$
$$Q(s) = q(s) \qquad s_n \leq s \leq 2\pi$$

then

$$\varphi_c(s) = \int_0^s Q(s)\, ds \qquad (5)$$

$$\Gamma_c = \int_0^{2\pi} Q(s)\, ds \qquad (6)$$
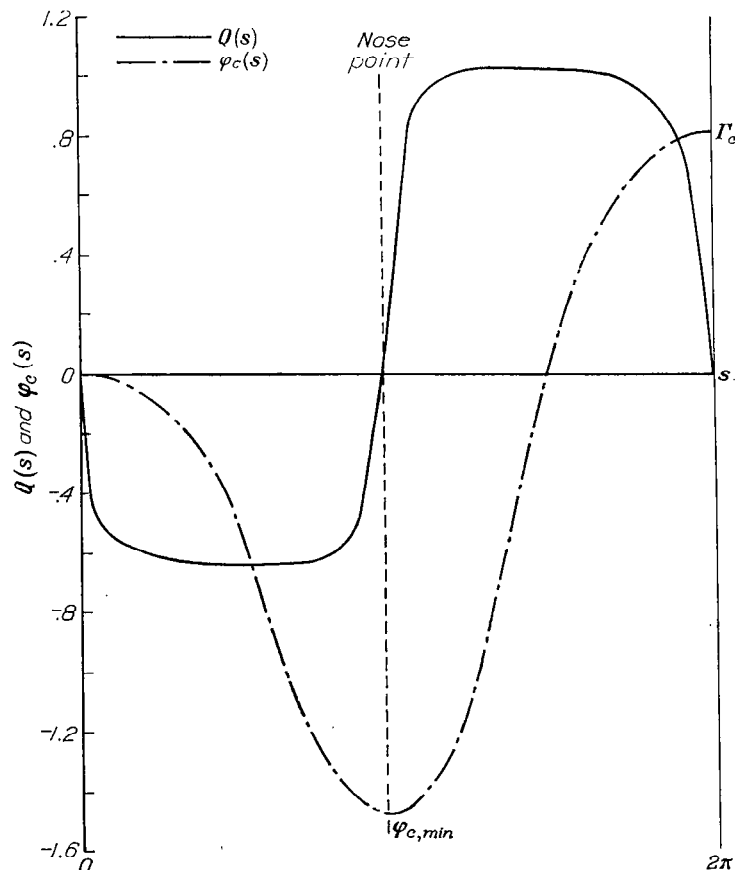
FIGURE 4.—Velocity and potential distribution for fluid with linear pressure-volume relation.

where the total arc length has been taken equal to 2π. These integrals are evaluated by Simpson's rule using sufficient points so as to obtain accurate values of $\varphi_c(s)$. The values of $\varphi_c(s)$ should be plotted on the graph with $Q(s)$ (fig. 4) in order to obtain q easily as a function of the circle angle later in the computation. The spacing d of the cascade is given by

$$d = \frac{\Gamma_c}{q_1 \sin \alpha_1 - q_2 \sin \alpha_2} \qquad (7)$$

From equation (35) of reference 1, the incompressible potential function for points on the unit circle may be written

$$\varphi_i(\theta) = -2\, Re\, A \tanh^{-1} \frac{\cos \theta}{\cosh k} + (Im\, A + Im\, B) \tan^{-1} \frac{\tan \theta}{\tanh k} +$$

$$(Im\, A - Im\, B) \tan^{-1} \frac{\sin \theta}{\sinh k} + D \qquad (8)$$

where D is chosen to make the potential zero at the tail stagnation point θ_t, the angle convention is $-\frac{\pi}{2} < \tan^{-1} \frac{\sin \theta}{\sinh k} < \frac{\pi}{2}$, and $\tan^{-1} \frac{\tan \theta}{\tanh k}$ is taken in the same quadrant and the same direction as θ. The values of $Re\, A$, $Im\, A$, $Re\, B$, and $Im\, B$ are determined from the free-stream conditions and spacing by

$$Re\, A = \frac{q_1 d\, |\cos \alpha_1|}{2\pi \sqrt{1 + q_1^2}} \qquad (9)$$

$$Im\, A = -\sqrt{1 + q_1^2}\, Re\, A \tan \alpha_1 \qquad (10)$$

$$Re\, B = -Re\, A \qquad (11)$$

$$Im\, B = \sqrt{1 + q_2^2}\, Re\, A \tan \alpha_2 \qquad (12)$$

The value of the constant k is determined by the condition that the potential range on the circle is equal to the potential range on the blade:

$$\varphi_c(2\pi) - \varphi_c(s_n) = \varphi_i(\theta_t + 2\pi) - \varphi_i(\theta_n) \qquad (13)$$

The proper value of k is computed by assuming a value for k and computing the stagnation points θ_t and θ_n, which are the roots of the equation

$$\sin(\theta + \lambda) = \frac{-(Im\, A + Im\, B) \sinh k}{2\, Re\, A \sec \lambda} \qquad (14)$$

where λ is given by

$$\lambda = \tan^{-1} \frac{(Im\, A - Im\, B) \tanh k}{2\, Re\, A} \qquad (15)$$

$$-\frac{\pi}{2} < \lambda < \frac{\pi}{2}$$

and then determining the value of $\varphi_i(\theta_t+2\pi)-\varphi_i(\theta_n)$. This process is repeated for different assumed values of k to obtain a plot of $\varphi_i(\theta_t+2\pi)-\varphi_i(\theta_n)$ as a function of k. The value of k satisfying equation (13) is then obtained by interpolation. A computational outline of this process for use with a desk calculator is given in table I, in which the usual column operations are written as lines.

When k has been determined, the flow about the circle is known with the value of the potential on the circle given by equation (8) and the velocity on the circle given by

$$v(\theta)=\frac{4\ Re\ A\cosh k\sec\lambda}{\cosh 2k-\cos 2\theta}\left[\sin(\theta+\lambda)-\sin(\theta_n+\lambda)\right]\quad(16)$$

A computational outline for $v(\theta)$ and $\varphi_i(\theta)$ based on 80 points is given in table II, lines 1 to 19.

DETERMINATION OF MAPPING FUNCTION

The mapping function (equation (62), reference 1) may be written in the form

$$z=\int\frac{4\ g_1{}^2-v(\theta)^2(2\cosh 2k-2\cos 2\theta)}{4\ g_1\ e^k\sqrt{2\cosh 2k-2\cos 2\theta}}e^{i\left(\theta+\frac{\pi}{2}+g_2-\tan^{-1}\frac{\sin 2\theta}{\cos 2\theta-e^{2k}}\right)}d\theta$$

$$(17)$$

where

$$g_1=[2-2\cos(\theta_t-\theta)]^{n/2}e^{[Re\ C(e^{i\theta})+(2\cosh 2k-2\cos 2\theta)\ Re\ H(e^{i\theta})]}$$

$$g_2=n\left(\frac{\pi+\theta_t-\theta}{2}\right)+Im\ C(e^{i\theta})+(2\cosh 2k-2\cos 2\theta)Im\ H(e^{i\theta})$$

and

$$n=1-\frac{\epsilon}{\pi}$$

where ϵ is the trailing-edge angle of the blade in radians. The mapping function is completely determined when $Re\ C(e^{i\theta})$, $Im\ C(e^{i\theta})$, $Re\ H(e^{i\theta})$, and $Im\ H(e^{i\theta})$ are known.

Determination of $Re\ C(e^{i\theta})$ and $Im\ C(e^{i\theta})$.—The function $C(e^{i\theta})$ is defined by equation (44) (reference 1) and may be written in the form

$$C(e^{i\theta})=\frac{1}{2}\left(1+e^{k-i\theta}\right)\ln\frac{Ae^{i\alpha_1+k}\left(1+\sqrt{1+q_1{}^2}\right)}{(1-e^{i\theta_t-k})^n q_1}+$$

$$\frac{1}{2}(1-e^{k-i\theta})\ln\frac{-Be^{i\alpha_2+k}\left(1+\sqrt{1+q_2{}^2}\right)}{(1+e^{i\theta_t-k})^n q_2}\quad(18)$$

Hence $Re\ C(e^{i\theta})$ and $Im\ C(e^{i\theta})$ are obtained by taking the real and imaginary parts of equation (18):

$$ReC(e^{i\theta})=\frac{1}{2}\left[(C_3+C_4)+e^k(C_3-C_4)\cos\theta+e^k(C_5-C_6)\sin\theta\right]\cdot$$

$$(19)$$

$$ImC(e^{i\theta})=\frac{1}{2}\left[(C_5+C_6)+e^k(C_5-C_6)\cos\theta-e^k(C_3-C_4)\sin\theta\right]$$

$$(20)$$

where

$$C_3=\ln\left\{\frac{1+\sqrt{1+q_1{}^2}}{q_1}\sqrt{Re^2A+Im^2A}\ e^k[e^{-k}(2\cosh k-2\cos\theta_t)]^{-n/2}\right\}$$

$$C_4=\ln\left\{\frac{1+\sqrt{1+q_2{}^2}}{q_2}\sqrt{Re^2B+Im^2B}\ e^k[e^{-k}(2\cosh k+2\cos\theta_t)]^{-n/2}\right\}$$

$$C_5=\tan^{-1}\left(\frac{Im\ A}{Re\ A}\right)+\alpha_1-n\tan^{-1}\left(\frac{-\sin\theta_t}{e^k-\cos\theta_t}\right)$$

$$C_6=\tan^{-1}\left(\frac{Im\ B}{Re\ B}\right)+\alpha_2-n\tan^{-1}\left(\frac{\sin\theta_t}{e^k+\cos\theta_t}\right)+\pi$$

The quadrants for the arc tangent terms in C_5 and C_6 are selected by considering the numerator and the denominator of the argument as signed quantities and choosing a quadrant in which the sine has the same sign as the numerator and the cosine has the same sign as the denominator. For convenience, these angles are taken as positive and the resulting values of C_5 and C_6 are changed by multiples of 2π until $|C_5|$ and $|C_6|$ are each less than 2π.

Determination of $Re\ H$ $(e^{i\theta})$.—In order to obtain $Re\ H$ $(e^{i\theta})$, the prescribed velocity along the blade must be determined as a function of the circle angle $q=q(\theta)$. This relation is obtained from the equality of the potentials at corresponding points in the two planes. Because $Q(s)$ and $\varphi_c(s)$ are plotted on the same graph (fig. 4), the magnitude of the prescribed velocity at a given circle angle θ may be found directly by reading the absolute value of Q $(q=|Q|)$ at the abscissa where $\varphi_c(s)$ equals the calculated value of $\varphi_i(\theta)$ (table II, line 19). The prescribed velocity is thus obtained as a function of the circle angle $q=q(\theta)$.

From equation (48) (reference 1)

$$Re\ H(e^{i\theta})=\frac{\ln\left[\frac{|v(\theta)|\sqrt{2\cosh 2k-2\cos 2\theta}}{K(\theta)\ [2-2\cos(\theta_t-\theta)]^{n/2}}\right]-Re\ C(e^{i\theta})+k}{2\cosh 2k-2\cos 2\theta}$$

$$(21)$$

where

$$K(\theta)=\frac{2q(\theta)}{1+\sqrt{1+q(\theta)^2}}\quad(22)$$

Lines 20 to 36 of table II show the detailed computation for obtaining $Re\ H(e^{i\theta})$, including the evaluation of $Re\ C(e^{i\theta})$.

Adjustment of $Re\ H(e^{i\theta})$.—Restrictions on the mapping function require that $Re\ H(e^{i\theta})$ satisfy the conditions

$$\int_{-\pi}^{\pi}Re\ H(e^{i\theta})\ d\theta=0\quad(23)$$

$$\int_{-\pi}^{\pi}Re\ H(e^{i\theta})\sin\theta\ d\theta=0\quad(24)$$

$$\int_{-\pi}^{\pi}Re\ H(e^{i\theta})\cos\theta\ d\theta=0\quad(25)$$

These integrals are evaluated numerically (in the manner developed by Dr. Glenn H. Peebles, while at Douglas Aircraft Co., Inc., in his work on isolated airfoils in incompressible flows) by using a parabolic variation of $Re\ H(e^{i\theta})$ between three consecutive points and integrating analytically. The point spacing used in the examples of this report is an equal spacing of 80 points (designated whole points and numbered 0, 1, 2, . . . 79) around the circle beginning with point 0 at $\theta = -180°$ and continuing around the circle at 4.5° intervals. Where $Re\ H(e^{i\theta})$ has large fluctuations (usually in the neighborhood of the stagnation points), the midpoints of these intervals (called half-points) are also used. The coefficients for evaluating the integral in equation (23) are the Simpson's rule coefficients. The coefficients for the integrals in equations (24) and (25), which are obtained by integrating analytically the product of the parabolas and $\sin\theta$ or $\cos\theta$, are given in tables III to VI. When half-interval spacing is used, it should begin and end at even-numbered points of the original 80 points and the integration coefficient to be used at the beginning (or ending) even-numbered point is one-half the sum of the whole-point coefficient and the half-point coefficient at that point.

If the values of $Re\ H(e^{i\theta})$ from equation (21) do not satisfy equations (23), (24), and (25), the velocity distribution chosen is incompatible with the chosen free-stream conditions and must be modified to make these integrals zero. The most desirable method of modification will depend on the magnitude of the integrals in equations (23), (24), and (25) and on the features of the original prescribed conditions that are to be preserved. Usually the original free-stream conditions are retained and the velocity distribution is modified. When the integrals are large, however, changing the circle flow may be desirable in order to minimize the changes in the essential characteristics of the original velocity distribution (such as limits on maximum velocity, diffusion rate, and so forth).

Modification of the circle flow provides essentially one additional degree of freedom, as can readily be seen from equations (9), (10), (11), and (12). The strength of the singularities A and B are determined by the free-stream conditions and the spacing. The range of potential is determined by the location of the singularities, that is, by the constant k. Only the ratio of the potential range to the spacing is important, however, because changing both together merely changes the dimensions of the cascade by a scale factor. This additional degree of freedom may be conveniently represented by the ratio of arc lengths of the upper and lower surfaces. Consequently, this ratio has a large influence on the size of the integrals in equations (23), (24), and (25). The selection of the ratio may be based on the ratio for a blade having a similar velocity distribution; or, in some cases, it may be advantageous to try several ratios of arc lengths and roughly approximate the integrals using only 20 points and from these results select the proper ratio to minimize these integrals. The final adjustment to reduce

these integrals to zero may then be obtained with a fixed circle flow by adjustment of $Re\ H(e^{i\theta})$.

When adjustments are being made in $Re\ H(e^{i\theta})$, the change in profile arc length and profile velocity $q(\theta)$ produced by these adjustments must be considered. The local arc length ds corresponding to $d\theta$ will be decreased in the same ratio that the velocity is increased in order to maintain the same potential. The change in arc length is automatically accounted for in the final integration for the blade coordinates. The change in the velocity produced by changing $Re\ H(e^{i\theta})$ by an amount $\Delta(Re\ H)$ is indicated by the change in the "distorted" velocity $K(\theta)$, which is related to $q(\theta)$ by equation (22) (fig. 5). The changed value, denoted by $\tilde{K}(\theta)$, is given by

$$\tilde{K}(\theta) = K(\theta)\, e^{-(2\cosh 2k - 2\cos 2\theta)\Delta(Re\ H)} \qquad (26)$$

Making a change in $Re\ H(e^{i\theta})$ therefore has the effect of multiplying the distorted velocity by a factor. This factor varies widely with the circle angle and produces the smallest change in $K(\theta)$ at $\theta = \pm\pi$ or $\theta = 0$ and the largest change at $\theta = \pm\pi/2$. Hence, for a given percentage change in $K(\theta)$, the greatest values of $\Delta(Re\ H)$ occur near $\theta = \pm\pi$ or $\theta = 0$. The effect of k on these values of $\Delta(Re\ H)$ for a given ratio of $\tilde{K}(\theta)/K(\theta)$ is shown in figure 6.

Consequently, for small values of the integrals in equations (23), (24), and (25), complete adjustment can frequently be made by merely changing the slope of the distorted velocity $K(\theta)$ at the stagnation points. The changes in the integrals produced by this change in slope are given by

$$\int_{-\pi}^{\pi} \Delta(Re\ H)\, d\theta$$

$$\int_{-\pi}^{\pi} \Delta(Re\ H)\, \sin\theta\, d\theta$$

$$\int_{-\pi}^{\pi} \Delta(Re\ H)\, \cos\theta\, d\theta$$
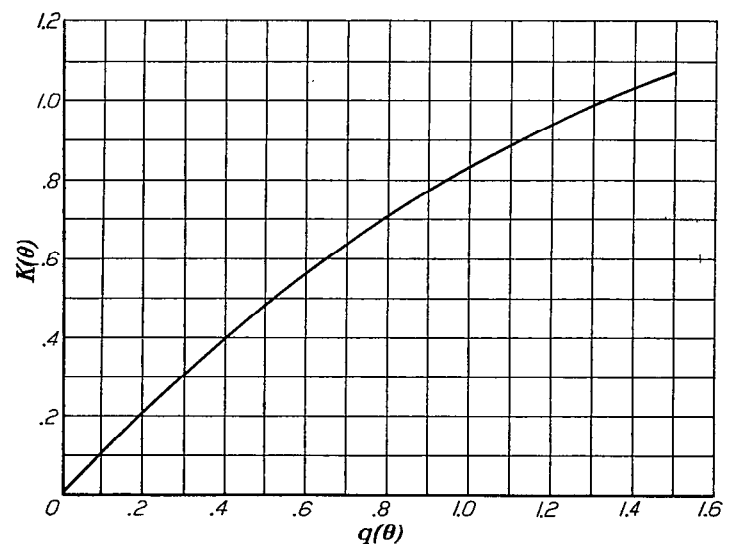
FIGURE 5.—Distorted velocity $K(\theta)$ as function of $q(\theta)$.

where $\Delta(Re\,H)$ is determined from equation (26). These changes in slope are effective in eliminating or reducing $\int Re\,H(e^{i\theta})\,d\theta$ and $\int Re\,H(e^{i\theta})\cos\theta\,d\theta$. (See figs. 6 and 7.)

Another method for adjusting $Re\,H(e^{i\theta})$ is to use a multiplier on the entire velocity distribution; that is,

$$\tilde{K}(\theta)=e^{-a}K(\theta)$$

then

$$\Delta(Re\,H)=\frac{a}{2\cosh 2k-2\cos 2\theta}$$

and

$$\int_{-\pi}^{\pi}\Delta(Re\,H)\,d\theta=\frac{a\pi}{\sinh 2k}$$

$$\int_{-\pi}^{\pi}\Delta(Re\,H)\sin\theta\,d\theta=0$$

$$\int_{-\pi}^{\pi}\Delta(Re\,H)\cos\theta\,d\theta=0$$

Changes in the sine and cosine integrals may be obtained by using different multipliers over the upper and lower surfaces:

$$\tilde{K}(\theta)=K(\theta)\,e^{-a_1}\qquad \theta_t\leq\theta\leq\theta_n$$

$$\tilde{K}(\theta)=K(\theta)\,e^{-a_2}\qquad \theta_n\leq\theta\leq\theta_t+2\pi$$

then

$$\Delta(Re\,H)=\frac{a_1}{2\cosh 2k-2\cos 2\theta}\qquad \theta_t\leq\theta\leq\theta_n$$

$$\Delta(Re\,H)=\frac{a_2}{2\cosh 2k-2\cos 2\theta}\qquad \theta_n\leq\theta\leq\theta_t+2\pi$$

and

$$\int_{-\pi}^{\pi}\Delta(Re\,H)d\theta=\left(\frac{a_1}{2\sinh 2k}\tan^{-1}\frac{\tan\theta}{\tanh k}\right)_{\theta_t}^{\theta_n}+$$
$$\left(\frac{a_2}{2\sinh 2k}\tan^{-1}\frac{\tan\theta}{\tanh k}\right)_{\theta_n}^{\theta_t+2\pi}$$

$$\int_{-\pi}^{\pi}\Delta(Re\,H)\sin\theta\,d\theta=-\left(\frac{a_1}{4\cosh k}\tanh^{-1}\frac{\cos\theta}{\cosh k}\right)_{\theta_t}^{\theta_n}-$$
$$\left(\frac{a_2}{4\cosh k}\tanh^{-1}\frac{\cos\theta}{\cosh k}\right)_{\theta_n}^{\theta_t+2\pi}$$

$$\int_{-\pi}^{\pi}\Delta(Re\,H)\cos\theta\,d\theta=\left(\frac{a_1}{4\sinh k}\tan^{-1}\frac{\sin\theta}{\sinh k}\right)_{\theta_t}^{\theta_n}+$$
$$\left(\frac{a_2}{4\sinh k}\tan^{-1}\frac{\sin\theta}{\sinh k}\right)_{\theta_n}^{\theta_t+2\pi}$$

These integrals may be easily evaluated because the inverse trigonometric functions all enter into the computation of $\varphi_i(\theta)$ and have been calculated in the determination of k.

A possibility for making small adjustments in $Re\,H(e^{i\theta})$ is to use a multiplier that is a simple function of θ, such as

$$\tilde{K}(\theta)=K(\theta)\,e^{-(a+b\cos\theta+c\sin\theta)}$$

then

$$\Delta(Re\,H)=\frac{a+b\cos\theta+c\sin\theta}{2\cosh 2k-2\cos 2\theta}$$

and

$$\int_{-\pi}^{\pi}\Delta(Re\,H)\,d\theta=\frac{a\pi}{\sinh 2k}$$

$$\int_{-\pi}^{\pi}\Delta(Re\,H)\sin\theta\,d\theta=\frac{c\pi(1-\tanh k)}{2}$$

$$\int_{-\pi}^{\pi}\Delta(Re\,H)\cos\theta\,d\theta=\frac{b\pi(1-\tanh k)}{2\tanh k}$$

Various combinations of these methods for adjustment of $Re\,H(e^{i\theta})$ have been used in the illustrative examples of this report.

After the adjustments in $Re\,H(e^{i\theta})$ have been made, the final values should be checked in equations (23), (24), and (25), as indicated in table II, lines 42, 43, and 44. At this time, $\tilde{K}(\theta)$ should be computed in order to determine whether $\tilde{K}(\theta)<2$, as required by part (d) of equation (5), reference 1. If $\tilde{K}(\theta)$ does not satisfy this inequality, a different modification of $Re\,H(e^{i\theta})$ is necessary.
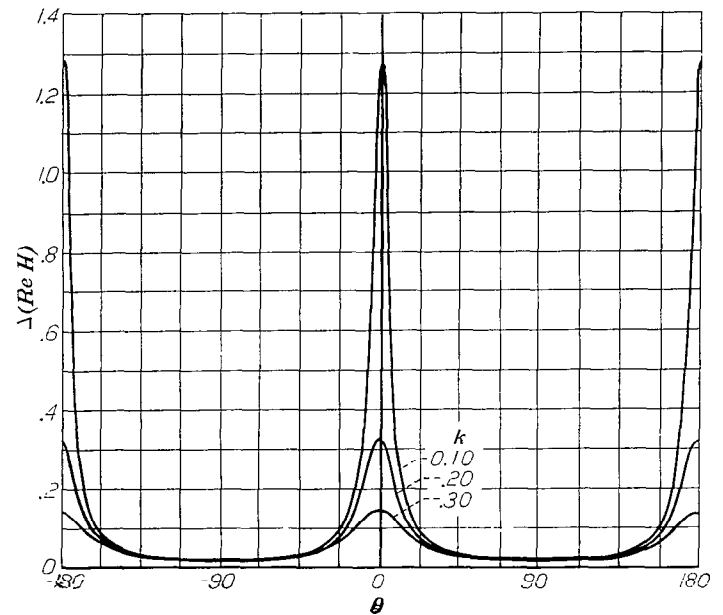
FIGURE 6.—$\Delta(Re\,H)$ as function of k and θ for ratio of distorted velocities $\tilde{K}(\theta)/K(\theta)=0.950$.
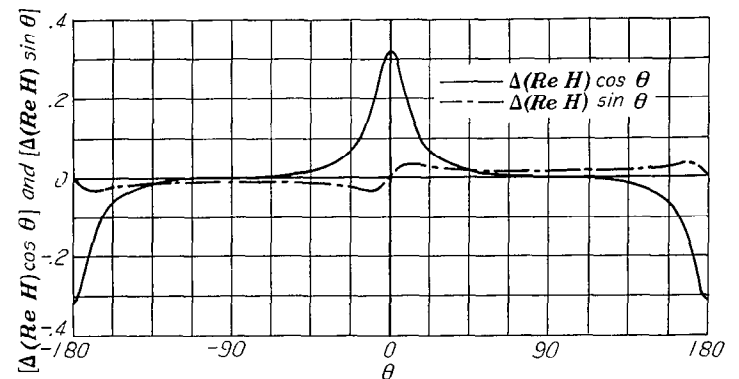
FIGURE 7.—Products $\Delta(Re\,H)\cos\theta$ and $\Delta(Re\,H)\sin\theta$ for $k=0.20$ and for $\tilde{K}(\theta)/K(\theta)=0.950$.

The final values of $Re\, H(e^{i\theta})$ and $\tilde{q}(\theta)$ should be plotted in order to insure that no excessive fluctuations have been introduced. At this time, $\tilde{q}(\theta)$ should be compared with the original $q(\theta)$ to make certain that the velocity has not been changed beyond acceptable limits. Because the potential range is fixed, these changes will change the arc length. If desired, $\tilde{q}(\theta)$ may be obtained as a function of the new arc length $\tilde{s}$ by

$$\tilde{q}(\theta)=\tilde{q}[\theta(\tilde{s})]=\tilde{q}(\tilde{s})$$

and

$$\tilde{s}(\theta)=\int_{\theta_i}^{\theta}\frac{|v(\theta)|}{\tilde{q}(\theta)}\,d\theta \qquad \theta_i\leq\theta\leq\theta_i+2\pi$$

The values of $\dfrac{|v(\theta)|}{\tilde{q}(\theta)}$ are given in table II, line 50.

Computation of $Im\,\tilde{H}(e^{i\theta})$.—When $Re\,\tilde{H}(e^{i\theta})$ satisfying all requirements has been obtained, the computation of the conjugate function $Im\,\tilde{H}(e^{i\theta})$ is done by direct numerical integration of Poisson's integral

$$Im\,\tilde{H}(e^{i\theta})=\frac{1}{2\pi}\int_{-\pi}^{\pi}Re\,\tilde{H}(e^{i\tau})\cot\frac{\tau-\theta}{2}\,d\tau$$

on the 80 basic points using an extension of the method developed by Dr. Glenn H. Peebles. The integration is accomplished by replacing $Re\,\tilde{H}(e^{i\theta})$ by 40 parabolas on the 80 basic points and integrating analytically the product of the parabolas and the cotangent term. The two sets of 80 coefficients so obtained for the integration are given in tables VII and VIII. (See appendix A for derivation.) The set in table VII is used for the computation of the conjugate at the end points of the parabolas; that is, at the even-numbered points 0, 2, 4, ... 78. The set in table VIII is used for the computation of the conjugate at the odd-numbered points 1, 3, 5, ... 79. Thus, to obtain $Im\,\tilde{H}(e^{i\theta})$ at one of the basic points, for example, point 7, the value of $Re\,\tilde{H}(e^{i\theta})$ at this point is multiplied by the first coefficient (0.000000) in table VIII, the next value of $Re\,\tilde{H}(e^{i\theta})$ (at point 8) is multiplied by the next coefficient (0.412368), and so forth, and the sum of these 80 products is the desired value of $Im\,\tilde{H}(e^{i\theta})$ at that point. Hence to obtain $Im\,\tilde{H}(e^{i\theta})$ at the 80 points requires 80 such accumulative multiplications. This computation is done very efficiently on an electronic calculating punch using only 415 cards and taking approximately 2 hours, including the time for key punching and verifying.

When $Re\,\tilde{H}(e^{i\theta})$ has large fluctuations so that some of the 80 basic intervals are divided by half-points, the preceding values of $Im\,\tilde{H}(e^{i\theta})$ must be corrected to take into account the difference between the values of $Re\,\tilde{H}(e^{i\theta})$ and the basic parabolas at these half-points. The correction to be added to the calculation is the harmonic conjugate of these differences. The coefficients for computing the value of the conjugate (at the 80 basic points) of these differences are given in table IX. (See appendix B.) This computation has been arranged on two concentric disks—the coefficients are carried by the outer disk and the differences (denoted by δ) are entered on the inner disk in the proper places (fig. 8). It is
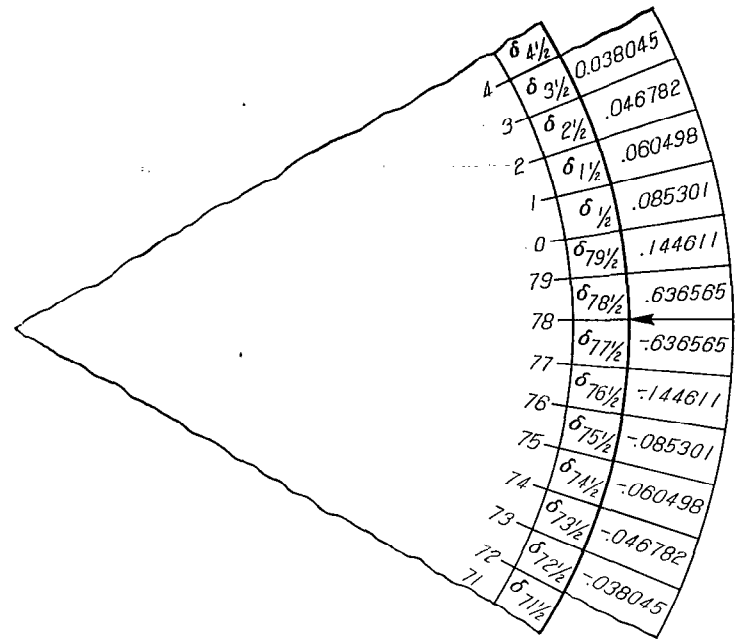
FIGURE 8.—Wheel for computing correction for $Im\,\tilde{H}(e^{i\theta})$. Indicated setting gives correction at point 78.

easy to see where these differences will make a significant contribution to $Im\,\tilde{H}(e^{i\theta})$ and to obtain the contribution by accumulative multiplication. This correction is then added to the calculated results.

COMPUTATION OF BLADE COORDINATES

After the corrected values of the conjugate have been obtained, the blade coordinates are given by equation (17), which for convenience of computation may be written in the parametric form

$$x(\theta)=\int_{-\pi}^{\theta}\frac{|v(\theta)|}{\tilde{q}(\theta)}\cos\left[\theta+\frac{\pi}{2}+g_2(\theta)-\tan^{-1}\frac{\sin 2\theta}{\cos 2\theta-e^{2k}}\right]d\theta \quad (27)$$

$$y(\theta)=\int_{-\pi}^{\theta}\frac{|v(\theta)|}{\tilde{q}(\theta)}\sin\left[\theta+\frac{\pi}{2}+g_2(\theta)-\tan^{-1}\frac{\sin 2\theta}{\cos 2\theta-e^{2k}}\right]d\theta \quad (28)$$

where

$$g_2(\theta)=n\left(\frac{\pi+\theta_i-\theta}{2}\right)+Im\,C(e^{i\theta})+(2\cosh 2k-$$

$$2\cos 2\theta)\,Im\,\tilde{H}(e^{i\theta})$$

These integrals are evaluated by Simpson's rule. In order to obtain sufficient accuracy, use of at least the same number of points as were used in the evaluation of $Re\,\tilde{H}(e^{i\theta})$ is advised. Because the values for $Im\,\tilde{H}(e^{i\theta})$ were calculated at the 80 basic points only, interpolation of $g_2(\theta)$ is necessary when half-points are used. The values of $x(\theta)$ and $y(\theta)$ are given in table II, lines 70 and 71.

EXAMPLES

Several examples have been computed to illustrate some of the variety of conditions to which the method may be readily applied. No attempt has been made to pick the

best velocity distribution or to obtain the *most desirable* blade shape, as to do so would lead to many considerations far beyond the scope of the present investigation.

In these examples, the adjustment of the prescribed velocity altered the arc length slightly. For uniformity, figures 9 to 12, which show the final velocity distribution and blade shape, were therefore scaled to give an arc length of 2π.

Example 1.—For this example of a cascade blade with low turning and a cusped trailing edge ($\epsilon=0$), the free-stream conditions were taken as

$$u_1=0.488 \qquad \alpha_1=170°$$

$$u_2=0.478 \qquad \alpha_2=180°$$

The velocity distribution prescribed on the blade was the velocity distribution for an isolated Joukowski airfoil. Adjustments to $Re\ H(e^{i\theta})$ altered this distribution somewhat and the resulting blade (which is very similar to a Joukowski airfoil) and velocity distribution are shown in figure 9.

Example 2.—For an example of an impulse-type blade with rounded leading and trailing edges ($\epsilon=\pi$), the free-stream velocities were assigned the values

$$u_1=0.555 \qquad \alpha_1=135°$$

$$u_2=0.555 \qquad \alpha_2=225°$$

and the prescribed velocity distribution on the blade was constant over most of the upper and lower surfaces with different values on the two surfaces and varied linearly

through the stagnation points. In this example, the expression for r (equation (4)) is indeterminate and the value of r was obtained by taking the limit as α_2 approaches 225°. In this example, complete adjustment of $Re\ H(e^{i\theta})$ was made by multiplying the velocities on the upper and lower surfaces by constants. The resulting blade shape and velocity distribution are shown in figure 10. A smaller nose or tail radius of curvature could be obtained by increasing the slope of the velocity distribution through the nose or the tail, respectively.

Example 3.—The free-stream velocities chosen for this example were representative of a compressor stage with

$$u_1=0.583 \qquad \alpha_1=135°$$

$$u_2=0.417 \qquad \alpha_2=155°$$

In order to keep the changes in the prescribed velocity to a minimum, three ratios of lower surface length to upper surface length of 0.95, 0.90, and 0.85 were used with the same prescribed velocity distribution (but, of course, different circle flows) and the integrals in equations (23), (24), and (25) were quickly approximated using only 20 points. By use of these results, a ratio that would give the smallest integrals was chosen (a ratio of 0.93) and the blade shape with rounded trailing edge ($\epsilon=\pi$) was computed in the usual manner.

FIGURE 9.—Final velocity distribution and blade shape for Example 1. $M_1=0.500$; $\epsilon=0$ (cusped trailing edge).
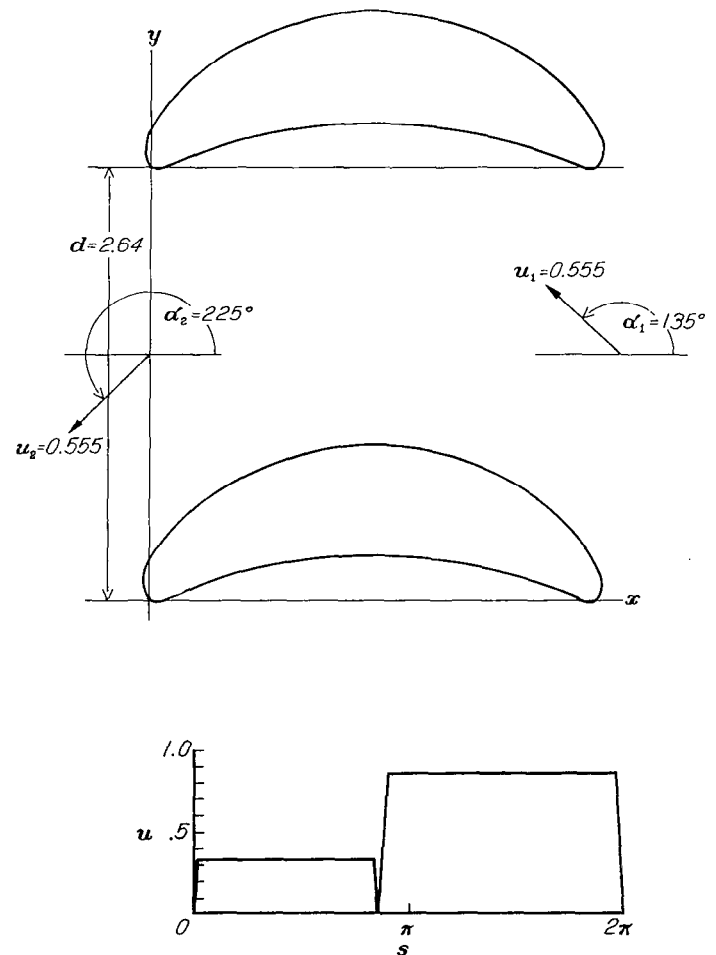
FIGURE 10.—Final velocity distribution and blade shape for Example 2. $M_1=0.573$; $\epsilon=\pi$ (rounded trailing edge).

The blade shape and the velocity distribution are shown in figure 11 (a). By use of the same circle flow and a change in $q(\theta)$, a blade having a 10° trailing-edge angle $\left(\epsilon=\dfrac{\pi}{18}\right)$ and similar velocity distribution was obtained (fig. 11 (b)).

Example 4.—In this example of a highly loaded cascade blade with a rounded trailing edge ($\epsilon=\pi$), the free-stream velocities were

$$u_1=0.579 \qquad \alpha_1=135°$$
$$u_2=0.369 \qquad \alpha_2=180°$$

The prescribed velocity distribution, which was similar to the distribution on a Griffith airfoil, had an abrupt decrease in value on the upper surface for use with suction. The blade and velocity distribution are shown in figure 12 (a). By use of the same circle flow and a change in $q(\theta)$, a blade having a cusped tail ($\epsilon=0$) and essentially the same velocity distribution was obtained (fig. 12 (b)).

DISCUSSION

Specification of the trailing-edge angle of the blade requires that $q(s)$ have a zero of order $\dfrac{\epsilon}{2\pi-\epsilon}$ at $s=0$ and $s=2\pi$. If the prescribed velocity does not go to zero in the proper manner,

$Re\,H(e^{i\theta})$ will be infinite at $\theta=\theta_t$. Fairing $Re\,H(e^{i\theta})$ smoothly through $\theta=\theta_t$ and keeping the values finite will, however, insure obtaining the specified angle at the trailing edge of the blade. The shape of the blade in the immediate vicinity of this point will depend on the velocity prescribed in this vicinity. If desired, the blade shape at the tail can easily be modified by changing $Im\,H(e^{i\theta})$, which changes the angle of the tangent to the blade (the angle in equations (27) and (28)). The corresponding change in $Re\,H(e^{i\theta})$ is computed from Poisson's integral with the constant term zero, and the modification in the velocity is obtained from this change in $Re\,H(e^{i\theta})$. The change in $Im\,H(e^{i\theta})$, denoted by $\Delta\,(Im\,H)$, should be chosen to satisfy the following conditions:

$$\int_{-\pi}^{\pi}\Delta(Im\,H)\,d\theta=0$$

$$\int_{-\pi}^{\pi}\Delta(Im\,H)\cos\theta\,d\theta=0$$

$$\int_{-\pi}^{\pi}\Delta(Im\,H)\sin\theta\,d\theta=0$$

For a prescribed velocity distribution requiring only moderate changes, the blade shape can be obtained in approximately 50 computing hours using 80 points and 4-decimal accuracy. The time depends, however, on the degree of familiarity with the method and on the extent of the permis-

(a) $\epsilon=\pi$ (rounded trailing edge).

(b) $\epsilon=\dfrac{\pi}{18}$ (10° trailing-edge angle).
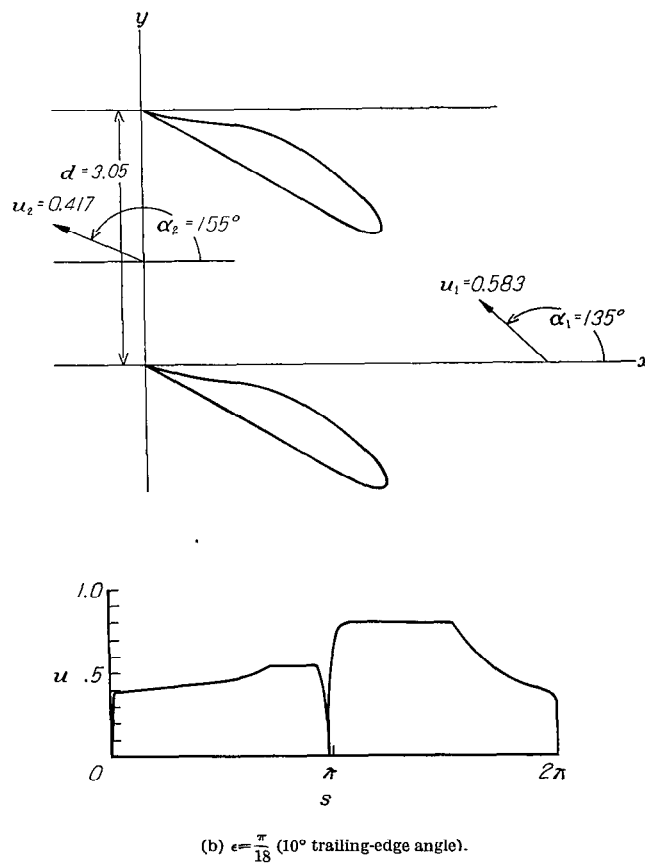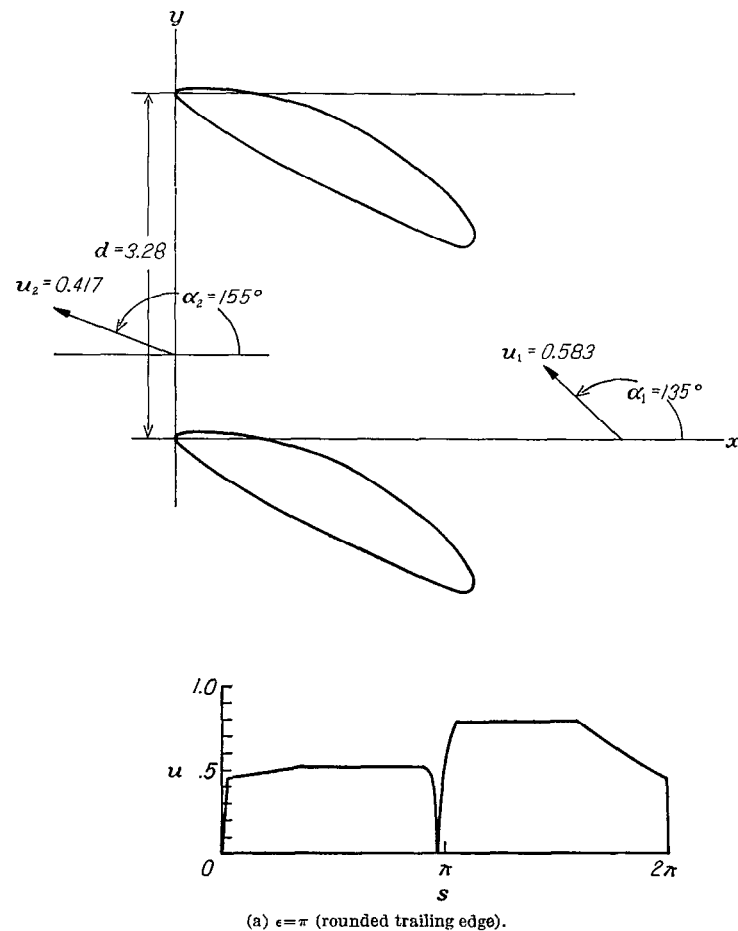
FIGURE 11.—Final velocity distribution and blade shape for Example 3. $M_1=0.604$.

(a) $\epsilon=\pi$ (rounded trailing edge).

(b) $\epsilon=0$ (cusped trailing edge).
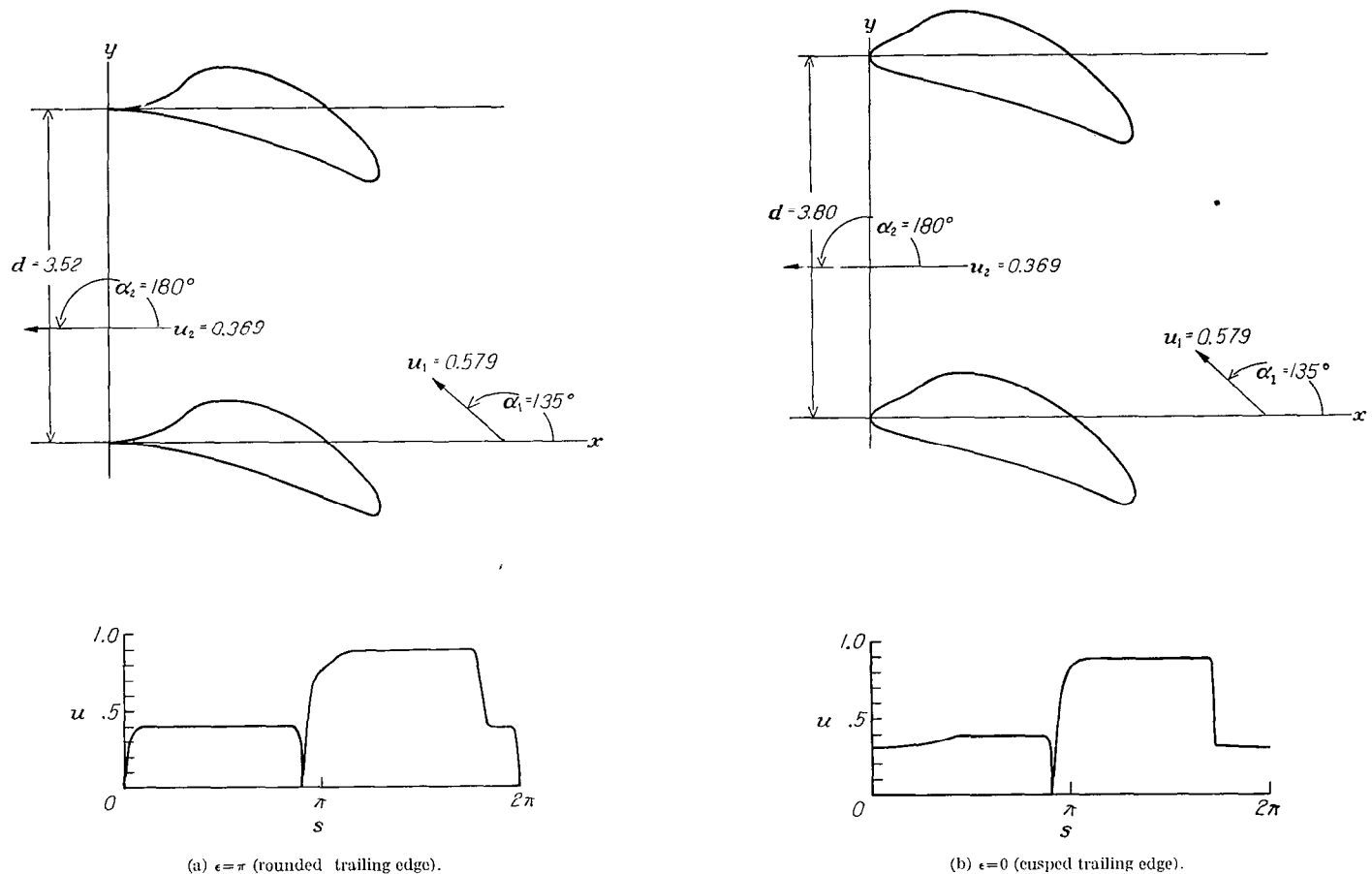
FIGURE 12.—Final velocity distribution and blade shape for Example 4. $M_1=0.599$.

sible modification to the velocity. When several examples have the same free-stream conditions and cascade spacing, the time is considerably reduced because the circle flow need be computed only once.

With the calculation based on a spacing of 80 points with half-points around the nose and the tail, the method gives accurate results in all cases in which the parameter k is not less than 0.10. Experience has shown that for cascades of moderate stagger and turning k will usually be greater than 0.10 when the solidity is less than 1. In examples 1, 2, 3, and 4, the values of k were 0.2600, 0.1100, 0.2008, and 0.2851 and the solidities were 0.91, 1.01, 0.92, and 0.74, respectively. In applying the method to other cases, a finer point spacing, which would require new coefficients for the integrations, should be used.

APPENDIX A

COEFFICIENTS FOR DETERMINING CONJUGATE FUNCTION

The coefficients for determining $Im\ H(e^{i\theta})$ are obtained by considering the contributions of one of the parabolas to the conjugate at one of the basic points. The contribution I of the $(k+1)$th parabola through the points $Re\ H(e^{i\theta_{2k}})$, $Re\ H(e^{i\theta_{2k+1}})$, and $Re\ H(e^{i\theta_{2k+2}})$ to the conjugate at any point $\theta=\theta_m$ is given by

$$I=\frac{1}{2\pi}\int_{\theta_{2k}}^{\theta_{2k+2}}[a(\theta-\theta_{2k+1})^2+b(\theta-\theta_{2k+1})+$$
$$Re\ H(e^{i\theta_{2k+1}})]\cot\frac{\theta-\theta_m}{2}\,d\theta$$

$$\text{(A1)}$$

where

$$a=\frac{Re\ H(e^{i\theta_{2k+2}})-2\ Re\ H(e^{i\theta_{2k+1}})+Re\ H(e^{i\theta_{2k}})}{2h^2}$$

$$b=\frac{Re\ H(e^{i\theta_{2k+2}})-Re\ H(e^{i\theta_{2k}})}{2h}$$

and h is the length of the basic interval. By substituting

$$\theta_{2k+1}=\theta_m+lh$$

in equation (A1) and expanding in series, equation (A1) can be integrated to give

$$I=R_l\,Re\ H(e^{i\,[(l-1)\,h+\theta_m]})+S_l\,Re\ H(e^{i\,(lh+\theta_m)})+$$
$$T_l\,Re\ H(e^{i\,[(l+1)\,h+\theta_m]})$$

where (for $l\neq 0,\ 1$)

$$R_l=\frac{1}{\pi}\left\{\left[\frac{1}{3}\left(\frac{h}{2}\right)^2+\frac{1}{15}\left(\frac{h}{2}\right)^4+\frac{2}{105}\left(\frac{h}{2}\right)^6+\frac{17}{2835}\left(\frac{h}{2}\right)^8+\cdots\right]-\right.$$
$$2\,(V_1L^2+V_2L^4+V_3L^6+\cdots)+4\,(W_1L+$$
$$\left.W_2L^3+W_3L^5+\cdots)\right\}$$

$$S_l=\frac{1}{\pi}\left[\ln\frac{\sin\frac{l+1}{2}h}{\sin\frac{l-1}{2}h}-8\,(W_1L+W_2L^3+W_3L^5+\cdots)\right]$$

$$T_l=\frac{1}{\pi}\left\{-\left[\frac{1}{3}\left(\frac{h}{2}\right)^2+\frac{1}{15}\left(\frac{h}{2}\right)^4+\frac{2}{105}\left(\frac{h}{2}\right)^6+\frac{17}{2835}\left(\frac{h}{2}\right)^8+\cdots\right]+\right.$$
$$2\,(V_1L^2+V_2L^4+V_3L^6+\cdots)+4\,(W_1L+$$
$$\left.W_2L^3+W_3L^5+\cdots)\right\}$$

and

$$L=\frac{\tan\frac{h}{2}}{\tan\frac{lh}{2}}$$

$$V_j=\left(\frac{\tan\frac{h}{2}}{h}\right)\left[-\frac{1}{(2j+1)}+\frac{1}{(2j+3)}\frac{\left(\tan\frac{h}{2}\right)^2}{3}-\right.$$
$$\frac{1}{(2j+5)}\frac{\left(\tan\frac{h}{2}\right)^4}{5}+\frac{1}{(2j+7)}\frac{\left(\tan\frac{h}{2}\right)^6}{7}-$$
$$\left.\frac{1}{(2j+9)}\frac{\left(\tan\frac{h}{2}\right)^8}{9}+\cdots\right]$$

$$W_j=\left(\frac{\tan\frac{h}{2}}{h}\right)^2\left[\frac{1}{(2j+1)}-\frac{1}{(2j+3)}\frac{2\left(\tan\frac{h}{2}\right)^2}{3}+\right.$$
$$\frac{1}{(2j+5)}\frac{23\left(\tan\frac{h}{2}\right)^4}{45}-\frac{1}{(2j+7)}\frac{44\left(\tan\frac{h}{2}\right)^6}{105}+$$
$$\left.\frac{1}{(2j+9)}\frac{563\left(\tan\frac{h}{2}\right)^8}{1575}-\cdots\right]$$

When $l=0$,

$$S_0=0$$

$$T_0=-R_0=\frac{1}{\pi}\left[1-\frac{1}{9}\left(\frac{h}{2}\right)^2-\frac{1}{225}\left(\frac{h}{2}\right)^4-\frac{2}{6615}\left(\frac{h}{2}\right)^6-\right.$$
$$\left.\frac{1}{42,525}\left(\frac{h}{2}\right)^8-\cdots\right]$$

When $l=1$,

$$S_1=\frac{4}{\pi}\left(\frac{1}{2}-\frac{h^2}{36}-\frac{h^4}{1350}-\frac{h^6}{26,460}-\frac{h^8}{425,250}-\cdots\right)$$

$$T_1=-\frac{1}{\pi}\left(\frac{h^2}{18}+\frac{2h^4}{675}+\frac{h^6}{8820}+\frac{4h^8}{212,625}+\cdots\right)$$

and R_1 is undefined because the integrand becomes infinite.

The final integration coefficients, denoted by N_0, N_1, N_2, ... are obtained from the preceding values of R_l, S_l, and T_l. When θ_m is an end point of a parabola (m is even), then

$$\left.\begin{aligned}N_0&=0\\N_1&=S_1\\N_2&=T_1+R_3\\&\cdots\\N_{2j-1}&=S_{2j-1}\\N_{2j}&=T_{2j-1}+R_{2j+1}\end{aligned}\right\}\quad\text{(A2)}$$

where N_0 is determined by Cauchy's principal value. When θ_m is a midpoint of a parabola (m is odd), then

$$\left.\begin{array}{l} N_0 = S_0 = 0 \\ N_1 = T_0 + R_2 \\ N_2 = S_2 \\ \quad \cdot \quad \cdot \quad \cdot \\ N_{2j-1} = T_{2j-2} + R_{2j} \\ N_{2j} = S_{2j} \end{array}\right\} \quad (A3)$$

The coefficients for 80 points given in tables VII and VIII were obtained from equations (A2) and (A3) using $h = 2\pi/80$. The coefficients for other point spacings can be obtained from equations (A2) and (A3) by using the proper value of h. Because of the symmetry of the coefficients, only half of them need be calculated.

APPENDIX B

COEFFICIENTS FOR CORRECTION OF CONJUGATE

The coefficients used in the wheel correction are obtained by determining the contribution of one of the half-point differences to the conjugate at one of the basic points. Denoting the contribution of the difference $\delta_{k+\frac{1}{2}}$ (the difference at $\theta = \theta_{k+\frac{1}{2}}$) to the conjugate at $\theta = \theta_m$ by I, then

$$I = \frac{1}{2\pi} \int_{\theta_k}^{\theta_{k+1}} \left[-\frac{4\delta_{k+\frac{1}{2}}}{h^2} (\theta - \theta_{k+\frac{1}{2}})^2 + \delta_{k+\frac{1}{2}} \right] \cot \frac{\theta - \theta_m}{2} \, d\theta$$

which, on substituting

$$\theta_{k+\frac{1}{2}} = \theta_m + \frac{h}{2} + lh$$

becomes

$$I = \frac{1}{2\pi} \int_{\theta_m + lh}^{\theta_m + (l+1)h} \left\{ -\frac{4\delta_{m+l+\frac{1}{2}}}{h^2} \left[\theta - \left(\theta_m + \frac{h}{2} + lh \right) \right]^2 + \delta_{m+\frac{1}{2}+l} \right\} \cot \frac{\theta - \theta_m}{2} \, d\theta \qquad (B1)$$

Integration of equation (B1) by series expansions gives (for $l \neq 0$)

$$I = \delta_{m+l+\frac{1}{2}} \frac{1}{\pi} \left[\ln \frac{\sin(l+1)\frac{h}{2}}{\sin\frac{lh}{2}} - 2(E_1 G + E_2 G^3 + E_3 G^5 + \ldots) \right]$$

where

$$G = -\frac{\tan\frac{h}{4}}{\tan(2l+1)\frac{h}{4}}$$

and

$$E_j = \left(\frac{4\tan\frac{h}{4}}{h} \right)^2 \left[\frac{1}{(2j+1)} - \frac{2\left(\tan\frac{h}{4}\right)^2}{3(2j+3)} + \frac{1}{(2j+5)} - \frac{23\left(\tan\frac{h}{4}\right)^4}{45} - \frac{1}{(2j+7)} \frac{44\left(\tan\frac{h}{4}\right)^6}{105} + \frac{1}{(2j+9)} \frac{563\left(\tan\frac{h}{4}\right)^8}{1575} - \ldots \right]$$

When $l = 0$,

$$I = \delta_{m+\frac{1}{2}} \frac{8}{\pi} \left(\frac{1}{4} - \frac{h^2}{288} - \frac{h^4}{43,200} - \frac{h^6}{3,386,880} - \ldots \right)$$

Consequently, the coefficients for the wheel correction denoted by $N_{\frac{1}{2}}$, $N_{1+\frac{1}{2}}$, $N_{2+\frac{1}{2}}$, . . ., are

$$N_{\frac{1}{2}} = \frac{8}{\pi} \left(\frac{1}{4} - \frac{h^2}{288} - \frac{h^4}{43,200} - \frac{h^6}{3,386,880} - \ldots \right)$$

$$N_{l+\frac{1}{2}} = \frac{1}{\pi} \left[\ln \frac{\sin(l+1)\frac{h}{2}}{\sin\frac{lh}{2}} - 2(E_1 G + E_2 G^3 + E_3 G^5 + \ldots) \right]$$

The coefficients in table IX, which are for 80 points, were obtained from equation (B2) using $h = 2\pi/80$. By use of other values of h in equation (B2), the coefficients for different point spacings can be obtained. Because of the symmetry of the coefficients, only half of them need be computed.

REFERENCE

1. Costello, George R.: Method of Designing Cascade Blades with Prescribed Velocity Distribution in Compressible Potential Flows. NACA Rep. 978, 1950. (Formerly NACA TN 1970.)

TABLE I—OUTLINE FOR COMPUTATION OF k

Line	Operation	Remarks
1	Assume a value of k	
2	sinh (1)	
3	cosh (1)	
4	tanh (1)	
5	$\frac{Im\ A - Im\ B}{2Re\ A} \times$ (4)	
6	$\tan^{-1}$ (5)	(6) is λ; express in degrees; $-90° < \lambda < 90°$
7	sec (6)	
8	$-\frac{(Im\ A + Im\ B)}{2Re\ A} \times \frac{(2)}{(7)}$	
9	$\sin^{-1}$ (8)	(9) is $\lambda + \theta_n$; $-90° \leq \lambda + \theta_n \leq 90°$
10	(9)$-$(6)	(10) is θ_n
11	$-$(10)$-$2(6)$-$180°	(11) is θ_t
12	(11)$+$360°	
13	sin (10)	
14	cos (10)	
15	tan (10)	
16	sin (12)	
17	cos (12)	
18	tan (12)	
19	(16)$\div$(2)	
20	(13)$\div$(2)	
21	(17)$\div$(3)	
22	(14)$\div$(3)	
23	(18)$\div$(4)	
24	(15)$\div$(4)	
25	$\tan^{-1}$ (19)	Express in radians; $-\frac{\pi}{2} < (25) < \frac{\pi}{2}$
26	$\tan^{-1}$ (20)	Express in radians; $-\frac{\pi}{2} < (26) < \frac{\pi}{2}$
27	$\tanh^{-1}$ (21)	
28	$\tanh^{-1}$ (22)	
29	$\tan^{-1}$ (23)	Express in radians; same quadrant and sign as $\theta_t + 2\pi$
30	$\tan^{-1}$ (24)	Express in radians; same quadrant and sign as θ_n
31	$(Im\ A - Im\ B) \times [(25)-(26)]$	
32	$-2Re\ A \times [(27)-(28)]$	
33	$(Im\ A + Im\ B) \times [(29)-(30)]$	
34	(31)$+$(32)$+$(33)	Must equal $\varphi_c(2\pi) - \varphi_c(s_n)$ for correct value of k

TABLE II—OUTLINE FOR COMPUTATION OF BLADE COORDINATES

Line	Operation	Remarks	Line	Operation	Remarks
1	Assign values of θ at 4.5° intervals beginning at $\theta = -\pi$	Half-points may be added later to these basic 80 points where necessary	40	$\Delta(Re\ H)$	Changes in $Re\ H(e^{i\theta})$ to make integrals zero; see text
2	2 (1)		41	(36)+(40)	(41) is $Re\ \tilde{H}(e^{i\theta})$
3	cos (2)		42	$\int_{-\pi}^{\pi}$ (41) $d\theta$	Must be zero
4	cosh 2k−(3)				
5	$(4Re\ A \cosh k \sec \lambda) \div (4)$	sec λ is line 7, table I	43	$\int_{-\pi}^{\pi}$ (41) sin $\theta\ d\theta$	Must be zero
6	(1)+λ	λ is line 6, table I			
7	sin (6)		44	$\int_{-\pi}^{\pi}$ (41) cos $\theta\ d\theta$	Must be zero
8	(7)−sin $(\theta_n + \lambda)$	sin $(\theta_n + \lambda)$ is line 8, table			
9	(8)×(5)	(9) is $v(\theta)$	45	$-(40)\times(29)$	
10	sin (1)		46	$e^{(45)}$	
11	cos (1)		47	(46)×(23)	(47) is $\tilde{K}(\theta)$; must have $\tilde{K}(\theta) < 2$ (equation (5d), reference 1)
12	tan (1)		48	4−(47)²	
13	(10)÷sinh k		49	4(47)÷(48)	(49) is $\tilde{q}(\theta)$
14	(11)÷cosh k				
15	(12)÷tanh k		50	|(9)|÷(49)	(50) is $\dfrac{d\tilde{s}}{d\theta}$
16	tan⁻¹ (13)	Express in radians; $-\dfrac{\pi}{2} < (16) < \dfrac{\pi}{2}$	51	$(C_5 - C_6)e^k \times (11)$	
17	tanh⁻¹ (14)		52	$(C_3 - C_4)e^k \times (10)$	
18	tan⁻¹ (15)	Express in radians; same quadrant and sign as θ	53	$[(C_5 + C_6) + (51) − (52)] \div 2$	(53) is $Im\ C(e^{i\theta})$
19	$(Im\ A − Im\ B) \times (16) − 2Re\ A \times (17) + (Im\ A + Im\ B) \times (18) + D$	(19) is $\phi_i(\theta)$ and $D = -(Im\ A − Im\ B) \tan^{-1} \dfrac{\sin \theta_t}{\sinh k} + 2Re\ A \tanh^{-1} \dfrac{\cos \theta_t}{\cosh k} − (Im\ A + Im\ B) \tan^{-1} \dfrac{\tan \theta_t}{\tanh k}$	54	Uncorrected $Im\ \tilde{H}(e^{i\theta})$	Obtained from machine calculation using coefficients in tables VIII and IX
			55	Correction for $Im\ \tilde{H}(e^{i\theta})$	Obtained from differences between $Re\ \tilde{H}(e^{i\theta})$ and parabolas using coefficients from table IX
20	$q(\theta)$	Obtain by matching potentials	56	(54)+(55)	(56) is $Im\ \tilde{H}(e^{i\theta})$
21	1+(20)²		57	$[(24)+180°]\times\dfrac{n}{2}$	(57)=0 when $n=0$
22	1+$\sqrt{(21)}$		58	(29)×(56)	
23	2 (20)÷(22)	(23) is the distorted velocity $K(\theta)$	59	57.29578 [(58)+(53)]	
24	θ_t−(1)		60	(57)+(59)	(60) is $g_2(\theta)$ in degrees
25	cos (24)	Omit these lines when $n=0$	61	sin (2)	
26	2−2 (25)		62	$(3)−e^{2k}$	
27	(26) $^{n/2}$	$n = \left(1 - \dfrac{\epsilon}{\pi}\right)$	63	(61)÷(62)	
28	(27)×(23)	(28) = (23) when $n=0$	64	tan⁻¹ (63)	Express as a positive angle in degrees; quadrant chosen so that sin (64) and cos (64) have same signs as (61) and (62), respectively
29	2 (4)		65	(1)+(60)+90°−(64)	
30	$\sqrt{(29)}$		66	cos (65)	
31	[(9)]×(30)÷(28)		67	sin (65)	
32	ln (31)		68	(50)×(66)	
33	$(C_5 - C_6)e^k \times (10)$		69	(50)×(67)	
34	$(C_3 - C_4)e^k \times (11)$				
35	$[(C_3 + C_4) + (33) + (34)] \div 2$	(35) is $Re\ C(e^{i\theta})$	70	$\int_{-\pi}^{\theta}$ (68) $d\theta$	(70) is $x(\theta)$; evaluate integral by Simpson's rule
36	$[(32)] − (35) + k] \div (29)$	(36) is $Re\ H(e^{i\theta})$			
37	$\int_{-\pi}^{\pi}$ (36) $d\theta$	Evaluate by Simpson's rule	71	$\int_{-\pi}^{\theta}$ (69) $d\theta$	(71) is $y(\theta)$; evaluate integral by Simpson's rule
38	$\int_{-\pi}^{\pi}$ (36) sin $\theta\ d\theta$	Evaluate by coefficients in tables III and V			
39	$\int_{-\pi}^{\pi}$ (36) cos $\theta\ d\theta$.	Evaluate by coefficients in tables IV and VI			

TABLE III—WHOLE-POINT COEFFICIENTS FOR SINE INTEGRAL

	0	10	20	30	40	50	60	70
0	0.00000	−0.03707	−0.05242	−0.03707	0.00000	0.03707	0.05242	0.03707
1	−.00821	−.07958	−.10433	−.06797	.00821	.07958	.10433	.06797
2	−.00820	−.04241	−.05178	−.03081	.00820	.04241	.05178	.03081
3	.02443	−.08923	−.10176	−.05468	.02443	.08923	.10176	.05468
4	−.01620	−.04671	−.04986	−.02380	.01620	.04671	.04986	.02380
5	−.04005	−.09669	−.09669	−.04005	.04005	.09669	.09669	.04005
6	−.02380	−.04986	−.04671	−.01620	.02380	.04986	.04671	.01620
7	−.05468	−.10176	−.08923	−.02443	.05468	.10176	.08923	.02443
8	−.03081	−.05178	−.04241	−.00820	.03081	.05178	.04241	.00820
9	−.06797	−.10433	−.07958	−.00821	.06797	.10433	.07958	.00821

TABLE IV—WHOLE-POINT COEFFICIENTS FOR COSINE INTEGRAL

	0	10	20	30	40	50	60	70
0	−0.05242	−0.03707	0.00000	0.03707	0.05242	0.03707	0.00000	−0.03707
1	−.10433	−.06797	.00821	.07958	.10433	.06797	−.00821	−.07958
2	−.05178	−.03081	.00820	.04241	.05178	.03081	−.00820	−.04241
3	−.10176	−.05468	.02443	.08923	.10176	.05468	−.02443	−.08923
4	−.04986	−.02380	.01620	.04671	.04986	.02380	−.01620	−.04671
5	−.09669	−.04005	.04005	.09669	.09669	.04005	−.04005	−.09669
6	−.04671	−.01620	.02380	.04986	.04671	.01620	−.02380	−.04986
7	−.08923	−.02443	.05468	.10176	.08923	.02443	−.05468	−.10176
8	−.04241	−.00820	.03081	.05178	.04241	.00820	−.03081	−.05178
9	−.07958	−.00821	.06797	.10433	.07958	.00821	−.06797	−.10433

TABLE V—HALF-POINT COEFFICIENTS FOR SINE INTEGRAL

	0	10	20	30	40	50	60	70
0	0.00000	−0.01852	−0.02619	−0.01852	0.00000	0.01852	0.02619	0.01852
½	−.00206	−.03844	−.05231	−.03554	.00206	.03844	.05231	.03554
1	−.00206	−.01991	−.01701	−.01701	.00206	.01991	.02611	.01701
1½	−.00615	−.04111	−.05199	−.03241	.00615	.04111	.05199	.03241
2	−.00410	−.02119	−.02587	−.01539	.00410	.02119	.02587	.01539
2½	−.01021	−.04353	−.05135	−.02908	.01021	.04353	.05135	.02908
3	−.00611	−.02233	−.02547	−.01368	.00611	.02233	.02547	.01368
3½	−.01421	−.04568	−.05039	−.02558	.01421	.04568	.05039	.02558
4	−.00809	−.02333	−.02491	−.01189	.00809	.02333	.02491	.01189
4½	−.01812	−.04754	−.04912	−.02192	.01812	.04754	.04912	.02192
5	−.01002	−.02419	−.02419	−.01002	.01002	.02419	.02419	.01002
5½	−.02192	−.04912	−.04754	−.01812	.02192	.04912	.04754	.01812
6	−.01189	−.02491	−.02333	−.00809	.01189	.02491	.02333	.00809
6½	−.02558	−.05039	−.04568	−.01421	.02558	.05039	.04568	.01421
7	−.01368	−.02547	−.02233	−.00611	.01368	.02547	.02233	.00611
7½	−.02908	−.05135	−.04353	−.01021	.02908	.05135	.04353	.01021
8	−.01539	−.02587	−.02119	−.00410	.01539	.02587	.02119	.00410
8½	−.03241	−.05199	−.04111	−.00615	.03241	.05199	.04111	.00615
9	−.01701	−.02611	−.01991	−.00206	.01701	.02611	.01991	.00206
9½	−.03554	−.05231	−.03844	−.00206	.03554	.05231	.03844	.00206

TABLE VI—HALF-POINT COEFFICIENTS FOR COSINE INTEGRAL

	0	10	20	30	40	50	60	70
0	−0.02619	−0.01852	0.00000	0.01852	0.02619	0.01852	0.00000	−0.01852
½	−.05231	−.03554	.00206	.03844	.05231	.03554	−.00206	−.03844
1	−.02611	−.01701	.00206	.01991	.02611	.01701	−.00206	−.01991
1½	−.05199	−.03241	.00615	.04111	.05199	.03241	−.00615	−.04111
2	−.02587	−.01539	.00410	.02119	.02587	.01539	−.00410	−.02119
2½	−.05135	−.02908	.01021	.04353	.05135	.02908	−.01021	−.04353
3	−.02547	−.01368	.00611	.02233	.02547	.01368	−.00611	−.02233
3½	−.05039	−.02558	.01421	.04568	.05039	.02558	−.01421	−.04568
4	−.02491	−.01189	.00809	.02333	.02491	.01189	−.00809	−.02333
4½	−.04912	−.02192	.01812	.04754	.04912	.02192	−.01812	−.04754
5	−.02419	−.01002	.01002	.02419	.02419	.01002	−.01002	−.02419
5½	−.04754	−.01812	.02192	.04912	.04754	.01812	−.02192	−.04912
6	−.02333	−.00809	.01189	.02491	.02333	.00809	−.01189	−.02491
6½	−.04568	−.01421	.02558	.05039	.04568	.01421	−.02558	−.05039
7	−.02233	−.00611	.01368	.02547	.02233	.00611	−.01368	−.02547
7½	−.04353	−.01021	.02908	.05135	.04353	.01021	−.02908	−.05135
8	−.02119	−.00410	.01539	.02587	.02119	.00410	−.01539	−.02587
8½	−.04111	−.00615	.03241	.05199	.04111	.00615	−.02908	−.05199
9	−.01991	−.00206	.01701	.02611	.01991	.00206	−.01701	−.02611
9½	−.03844	.−00206	.03554	.05231	.03844	.00206	−.03554	−.05231

TABLE VII—COEFFICIENTS FOR CONJUGATE AT EVEN-NUMBERED POINTS

	0	10	20	30	40	50	60	70
0	0.000000	0.020031	0.008323	0.003449	0.000000	−0.003449	−0.008323	−0.020031
1	.636402	.036217	.015415	.006151	−.000655	−.007686	−.018042	−.045294
2	.050356	.016305	.007110	.002706	−.000655	−.004243	−.009743	−.025472
3	.144119	.029799	.013146	.004702	−.001973	−.009338	−.021159	−.059345
4	.050944	.013568	.006049	.001999	−.001319	−.005102	−.011449	−.034277
5	.084480	.024968	.011141	.003316	−.003316	−.011141	−.024968	−.084480
6	.034277	.011449	.005102	.001319	−.001999	−.006049	−.013568	−.050944
7	.059345	.021159	.009338	.001973	−.004702	−.013146	−.029799	−.144119
8	.025472	.009743	.004243	.000655	−.002706	−.007110	−.016305	−.050356
9	.045294	.018042	.007686	.000655	−.006151	−.015415	−.036217	−.636402

TABLE VIII—COEFFICIENTS FOR CONJUGATE AT ODD-NUMBERED POINTS

	0	10	20	30	40	50	60	70
0	0.000000	0.040322	0.016677	0.006906	0.000000	−0.006906	−0.016677	−0.040322
1	.412368	.018011	.007694	.003072	−.000327	−.003839	−.009002	−.022467
2	.223706	.032759	.014242	.005417	−.001312	−.008495	−.019528	−.051462
3	.065520	.014841	.006563	.002349	−.000986	−.004663	−.010554	−.029282
4	.106592	.027228	.012115	.004003	−.002641	−.010218	−.022960	−.069820
5	.041111	.012446	.005563	.001657	−.001657	−.005563	−.012446	−.041111
6	.059820	.022960	.010218	.002641	−.004003	−.012115	−.027228	−.106592
7	.029282	.010554	.004663	.000986	−.002349	−.006563	−.014841	−.065520
8	.051462	.019528	.008495	.001312	−.005417	−.014242	−.032759	−.223706
9	.022467	.009002	.003839	.000327	−.003072	−.007694	−.018011	−.412368

TABLE IX—COEFFICIENTS FOR CORRECTION TO CONJUGATE

	0	10	20	30	40	50	60	70
0	0.636565	0.019061	0.008014	0.003262	−0.000164	−0.003645	−0.008669	−0.021304
1	.144611	.017188	.007406	.002890	−.000492	−.004042	−.009379	−.024049
2	.085301	.015596	.006840	.002528	−.000821	−.004455	−.010156	−.027496
3	.060498	.014222	.006309	.002175	−.001153	−.004885	−.011011	−.031974
4	.046782	.013021	.005809	.001829	−.001488	−.005335	−.011960	−.038045
5	.038045	.011960	.005335	.001488	−.001829	−.005809	−.013021	−.046782
6	.031974	.011011	.004885	.001153	−.002175	−.006309	−.014222	−.060498
7	.027496	.010156	.004455	.000821	−.002528	−.006840	−.015596	−.085301
8	.024049	.009379	.004042	.000492	−.002890	−.007406	−.017188	−.144611
9	.021304	.008669	.003645	.000164	−.003262	−.008014	−.019061	−.636565